

## Fast optical monitoring of microscopic excitation patterns in cardiac muscle

W. Müller, H. Windisch, H. A. Tritthart

Institut für Medizinische Physik und Biophysik, A-8010 Graz, Austria

**ABSTRACT** Many vital processes depend on the generation, changes, and conduction of cellular transmembrane potentials. Optical monitoring systems are well suited to detect such cellular electrical activities in networks of excitable cells and also tissues simultaneously at multiple sites.

Here, an exceptionally fast array system ( $16 \times 16$  photodiodes, up to 4,000,000 samples per second, 12-bit resolution) for imaging voltage-sensitive dye fluorescence, permitted real time measurements of excitation patterns at a microscopic size scale (256 pixels within an area of  $1.8\text{--}8\text{ mm}^2$ ), in

rat cardiac muscle in vitro. Results emphasize a recent hypothesis for cardiac impulse conduction, based on cardiac structural complexities, that is contradictory to all continuous cable theory models.

### INTRODUCTION

Many dyes, bound to cell membranes, respond to changes in electrical field strength by altering their fluorescence light intensity. This effect has been applied to measure membrane potential changes in various excitable tissues (1–4). Fluorescence monitoring of electrical cell activity shows important advantages when compared with microelectrode techniques: no impalement artefacts, precise selection of both the size and location of the measuring spot, and simultaneous monitoring of many cells or groups of cells. Temporal and spatial resolutions are comparable or even superior to those obtained using microelectrode techniques (5, 6). The large number of available voltage-sensitive dyes enables the experimentalist to select the one which shows large signals and minimum toxic or photodynamic effects in the specimen under study. Signal-to-noise ratios of optically detected membrane potential changes were remarkably increased during the last decade, however, the smooth traces and the eased voltage calibration known from microelectrode techniques are not reached yet.

The systems which have been reported for optical multisite detection of membrane potentials fall into three basic types: photodiode array systems, laser scanning systems, and video systems (7–17). With time resolutions typically in the range of milliseconds, none of them are capable of monitoring the spread of excitation in quickly propagating networks, e.g., nerve tissue or mammalian heart muscle, with microscopic spatial resolution over macroscopic areas.

### MATERIALS AND METHODS

We have designed a new photodiode array system (Fig. 1) consisting of a  $16 \times 16$  rectangular grid of low-cost photodiodes (type BPW 34), 256

amplifiers, and a fast, cascaded multiplexing unit which feeds a four-channel digital storage oscilloscope (maximum 1 MHz sampling and 16 kilobyte memory on each channel). A total data throughput of 4,000,000 data values per second with 12-bit resolution has been achieved. This system permits real-time monitoring of the spread of excitation in rat myocardium at a size scale well matched to the dimensions of cardiac muscle fibers and fiber bundles; the distance between pixels is either 84 or 180  $\mu\text{m}$ , depending on the choice of optics (Olympus A 20/0.40 or Olympus SPLAN 10/0.30, both converted to pseudo-water immersion). The numerical apertures of the objectives were enhanced because we used shorter working distances than normal.

An argon ion laser (514 nm, 0.5–2 W; COHERENT INNOVA 90/4) was used to excite fluorescence of the di-4-ANEPPS-stained cardiac tissue (4, 18). The laser beam was switched with an optical shutter (Pockels cell). The fluorescent light of the area imaged on the array was simultaneously sensed by the 256 photodiodes. The current signals were converted to voltages (rise time of the current-to-voltage amplifiers was 140  $\mu\text{s}$ ) and fed through two levels of cascaded 16-channel analog multiplexers (HEF4067BP) to produce either four or a single output signal. In four-channel mode, each output was stored in one-channel memory of the externally synchronized digital oscilloscope (W & W Recorder 112.124, Basel, Switzerland). The time-base frequency was 0.5 or 1 MHz in the experiments shown here; this produced an effective sample rate for each photodiode of 7.8 or 15.6 kHz, respectively. For other possible applications of this system the time-base frequency can be lowered down to 125 kHz, thus action potential propagation can be continuously monitored for 128 ms ( $4 \times 16$  kilobyte memory) in this case. For the investigation of fast phenomena separated by periodic time intervals, the system can be operated intermittently. The experimentalist can choose a number of cycles up to 99 and a duration of the interruption between 10 and 990 ms in this mode. Beyond that, the availability of a larger memory will increase the number of possible applications.

Stored data was transferred by IEEE-488 interface bus from the digital oscilloscope to a central minicomputer (HP 1000/A 900) for offline processing (5). Before each measurement the specimen was focused precisely by means of conventional video techniques. Additionally, the video image was digitally stored and superimposed onto the pattern of electrical activity for topographic orientation. Preliminary aspects of parts of this system were presented in 1987 (19).

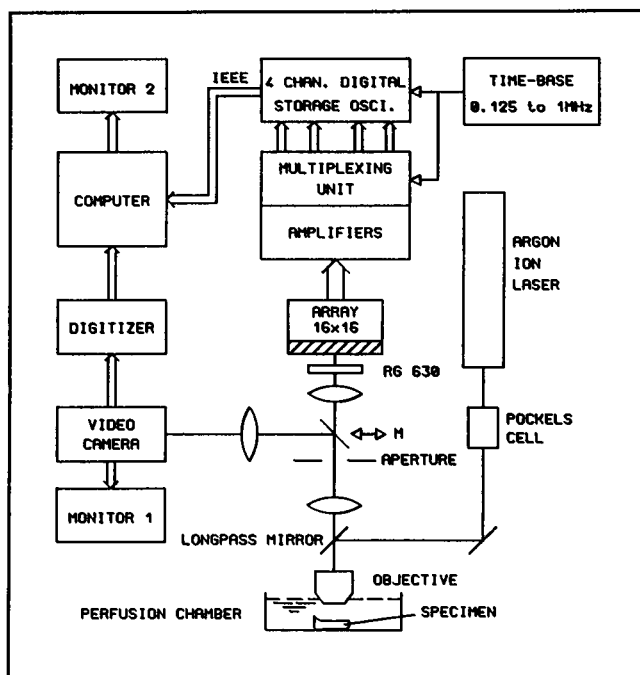


**FIGURE 1** The schematic diagram shows the outline of a photodiode array system, designed for measurements of the spread of electrical excitation in microscopically small areas of biological tissues stained with a voltage-sensitive dye. The monitored area of the specimen was  $2.8 \times 2.8 \text{ mm}^2$  or  $1.35 \times 1.35 \text{ mm}^2$ , depending on the objective inserted. An aperture ( $16 \times 16 \text{ mm}^2$ ) was situated in the first, the photodiode array ( $16 \times 16$  rectangular grid of BPW34 photodiodes) in the second image plane. Backscattered light was cut off by the filter RG 630 (Schott Glass Technologies Inc., Duryea, PA). The argon ion laser (514 nm, 0.5–2 W) was used to excite fluorescence of the stained tissue. The beam was switched with a Pockels cell. Photodiode currents were amplified and converted to voltage and then fed to a cascaded multiplexing unit. In a first step the 256 signals were compressed to 16 (16 HEF4067BP analogue selectors were applied). In a second step these 16 outputs were converted to either one or four signals. Correspondingly one or four analog selectors, which were operated at  $1/4$  of the actual time-base frequency, were applied in this second part of the multiplexing unit. A total data throughput of 4,000,000 data values per second has been achieved in the fastest mode (four output signals synchronously, 1 MHz time-base frequency) and data was stored in the memory of a four-channel digital storage oscilloscope (12-bit resolution) which functioned as an analog-to-digital converter and as a fast temporary digital storage. The oscilloscope was externally synchronized with a delayed time-base signal (variable delay time was 50–90% of the time-base period). Stored multiplexed data was transferred via IEEE-interface to the minicomputer HP1000/A900. Moving the mirror M into the optical path permitted visual control of the magnified specimen on screen 1. A digital video image ( $128 \times 128$  pixels) was stored and superimposed onto the pattern of electrical activity displayed on the screen of monitor 2.

We applied this newly finished technique to study the propagation of excitation in  $1.8\text{--}8 \text{ mm}^2$  areas of papillary muscle and atrial sheets (auricles) of the rat heart. Excised specimens were stained for 10 min at room temperature (di-4-ANEPPS-saturated ethanol stock solution diluted with Tyrode solution by 100–200), and thereafter placed in a

tissue bath and superfused with dye-free Tyrode solution at  $37^\circ\text{C}$  (6). Fluorescence microscopy demonstrated that only one or two surface cell layers were stained with potential sensitive dye. This was expected before (5), otherwise optical membrane potential measurements would not be as fast or even faster than microelectrode measurements, due to superimposing effects. The preparation was stimulated externally at 1 Hz frequency throughout the experiment. Both, atrial sheets and papillary muscle, showed high fractional changes in fluorescence light intensity,  $\Delta F/F$ , of up to 9%, due to the action potential amplitude, which is typically 100 mV in rat myocardium. The amplitude of the fluorescence signal varied in different regions. The smallest signals evaluated showed changes in fluorescence light intensity of  $\sim 1\%$ .

Usually several consecutive measurements were performed to compare, but not to average, the results. In a control experiment with the papillary muscle of Fig. 2, for example, we compared the time courses of all 96 photodiode signals that showed an action potential, with the corresponding traces from a subsequent measurement. This was repeated three times, thus  $n$  was 288. The deviation in the arrival time of the action potential upstrokes, measured during two subsequent heart beats, was within  $\pm 130 \mu\text{s}$  in 72%, within  $\pm 260 \mu\text{s}$  in 90%, and within  $\pm 390 \mu\text{s}$  in 98% of all cases. These small deviations in time were partly due to biological instability (mechanical motion, etc.) and partly due to the laser noise in the range of 0.3–0.5% peak-to-peak. Signal-to-noise ratios were typically in the range of 5:1 to 25:1 (peak-to-peak). The cross-talk between the channels was negligible.

## RESULTS

Spread of excitation across the imaged area of the papillary muscle is shown in Fig. 2. The color-coded map was constructed by timing the arrival of the optically monitored upstroke of the action potentials; maxima of inverted first time derivatives  $-dF/dt$  of the fluorescence signals  $F(t)$  were used to indicate the arrival time of propagated excitation for each pixel ( $F$  decreased as the membrane potential  $V$  increased). Those pixels, in which the  $-dF/dt$  maxima occurred in the same given time interval were coded with the same color. Propagation proceeded with high velocity from the lower right side (close to the position of the stimulus electrode) in the longitudinal direction (green followed by yellow and so on) and much more slowly in the transverse direction (several windows of the color code are skipped). In Fig. 3 *a*, maxima of  $-dF/dt$  from photodiodes arranged in the direction of fiber orientation are closer to each other than those from signals of pixels joined in a transverse direction (Fig. 3 *b*), thus indicating the difference in propagation velocity. Conduction velocities were estimated by dividing the distance between two pixels by the difference in time at which maximum  $-dF/dt$  occurred at each pixel.

With regard to the discussion on discontinuous conduction which follows, note that there was no delayed propagation of the action potential in a longitudinal direction on the left side of the preparation (see Fig. 2). Otherwise this could have caused the time delays in the border zone, where yellow coded pixels adjoin violet and blue ones.

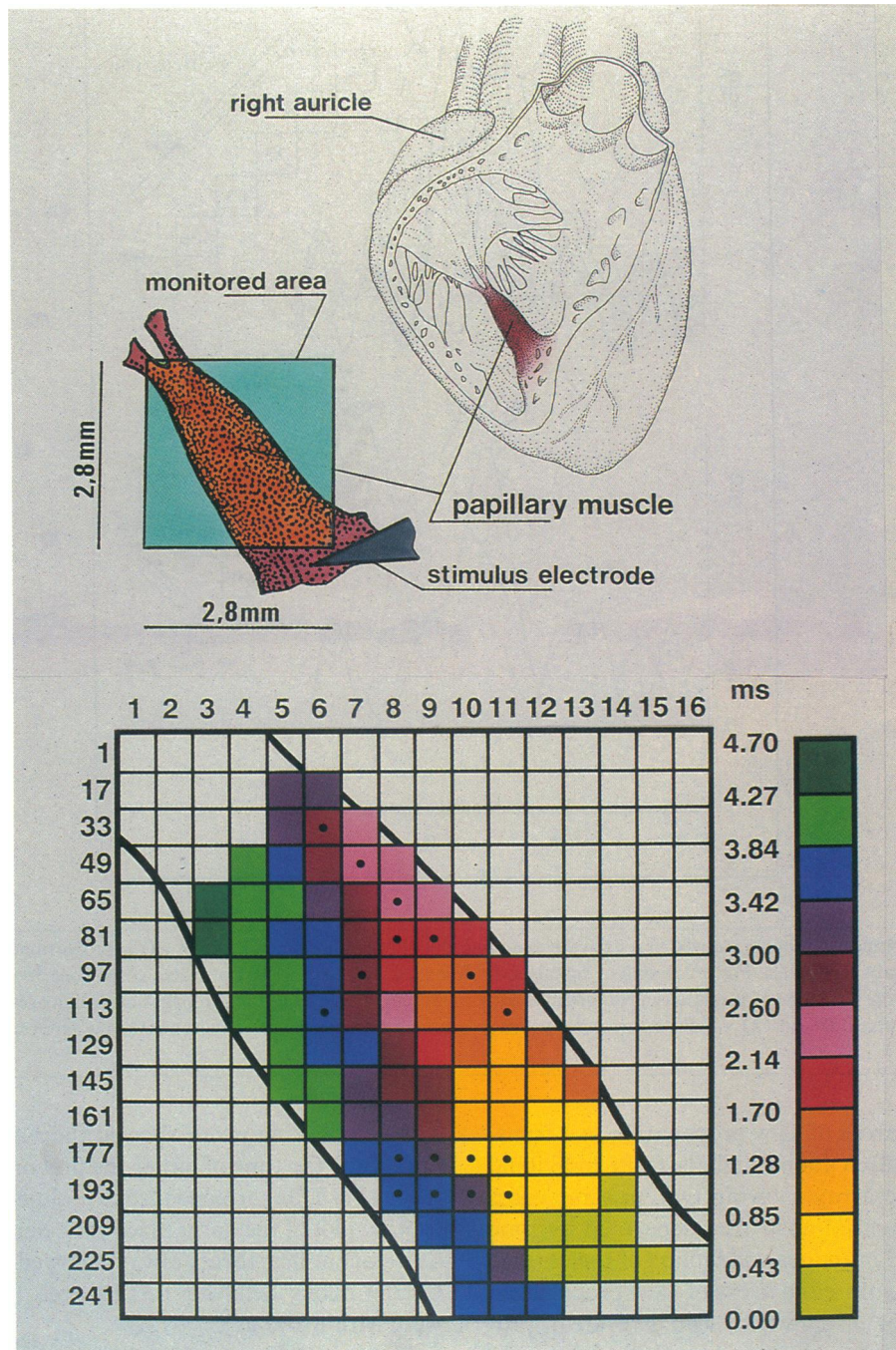


**FIGURE 2** Fluorescence real-time monitoring of the microscopic excitation pattern in a rat papillary muscle, which was stained with the potential sensitive dye di-4-ANEPPS. After staining the specimen was placed in a tissue bath and superfused with pH-balanced Tyrode solution at 37°C. The pattern shown was constructed by timing the optically monitored incidence of propagated excitation. Maxima of  $-dF/dt$  (corresponding to the occurrence time of maximum  $dV/dt$ ,  $V$  being the membrane potential) were taken as fiducial points of this incidence, and those areas where maxima occurred in a given time interval were coded with the same color. Numbers on left side of the squared frame indicate the first pixel number of the line. Propagation proceeded with high velocity from the lower right side in the longitudinal direction and slowly in the transverse direction. For estimated velocity values of dotted strings of pixels, see Fig. 3. A discontinuous conduction phenomenon was found, for example, in the dotted zone in and around pixel 186. Plots of the signals of the associated photodiodes are shown in Fig. 4.

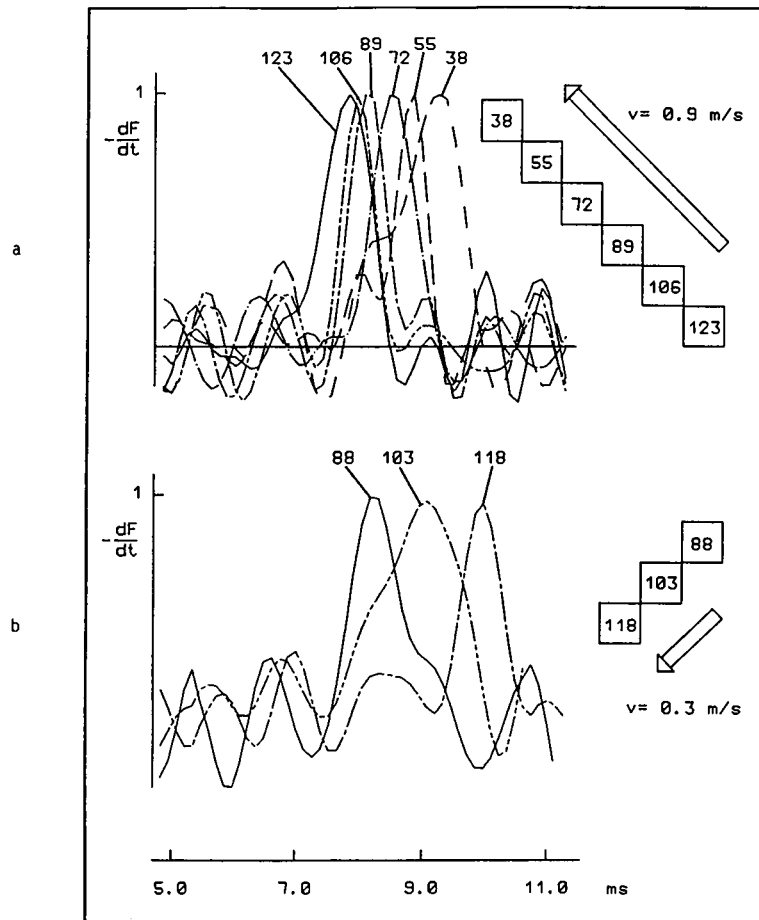
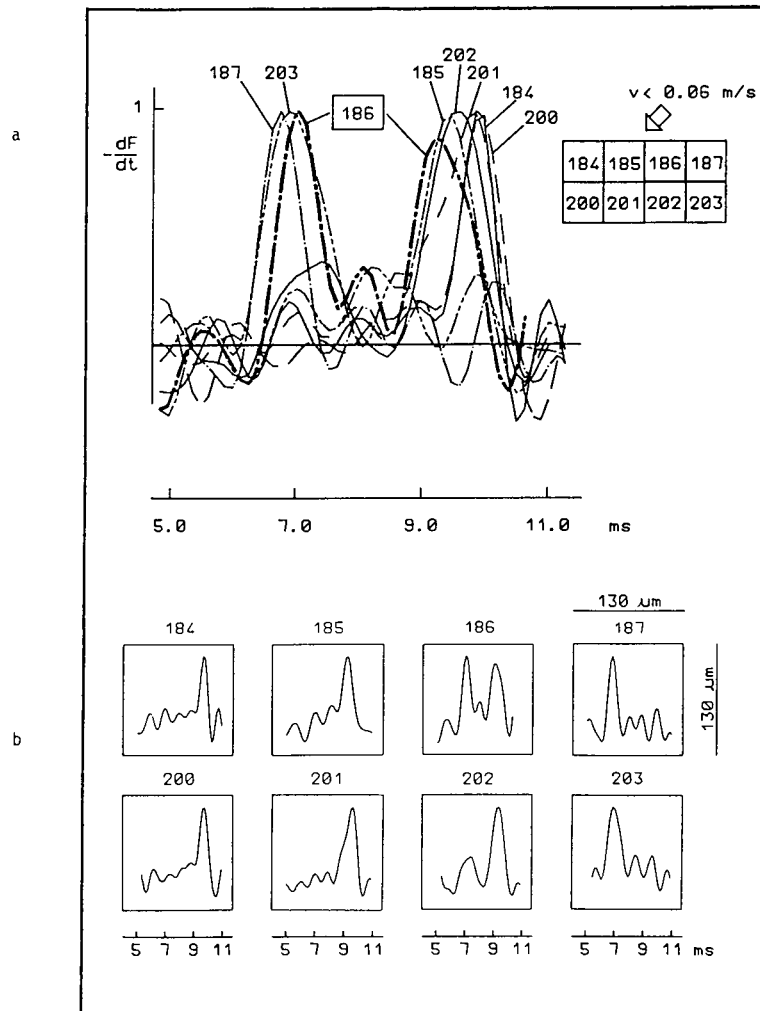


FIGURE 3 Time-course comparisons of normalized first derivatives of digitally filtered fluorescence signals  $F(t)$  (proportional to the action potential upstroke velocities) from adjacent pixels. For processing of signals see reference 5 and 6. Numbers of traces correspond to pixel numbers in Fig. 2. Pixel size was  $180 \times 180 \mu\text{m}^2$ . (a) Line of pixels arranged longitudinally to muscle fiber orientation. Propagation velocity of activation was 0.9 m/s, calculated from signals of pixels 38 and 123. (b) Pixels arranged transverse to fiber orientation; velocity was 0.30 m/s here (evaluated from signals 88 and 118).

Predominantly in areas of slow propagation in a transverse direction, we often found signals from individual photodiodes from the array showing two, in some cases even three action potential upstrokes, separated by time delays up to 2.5 ms. Continuous conduction of the cardiac impulse, optically monitored in areas of slow propagation transverse to the fiber orientation, would result in prolonged action potential upstrokes, but never in two or more separated action potential onsets from neighboring fibers within areas of the size of single pixels. We found a discontinuous kind of propagation, for example, at the site of pixel 186 and in its neighborhood where the yellow coded area adjoins the violet one in the pattern in Fig. 2. The time course of the signal of photodiode 186 showed two action potential upstrokes, separated by a time lag of 2.2 ms. Correspondingly, two peaks in the plot of the negative first time derivative were found (Fig. 4, *a* and *b*).

The neighboring pixels showed their maxima in  $-dF/dt$  at (about) the time of either the first or the second peak in trace 186. This correspondence in time is pointed out in an overlay plot of the normalized time derivatives in Fig. 4 *a*. Subsequent heartbeats always showed precisely the same discontinuous behavior in this area (deviations in time were within  $200 \mu\text{s}$ ).

Not only did we find discontinuous spread of excitation in the direction transverse to the fiber orientation in papillary muscle, but, in one case, also in the longitudinal direction. Even at a pixel size of only  $60 \times 60 \mu\text{m}^2$  we found signals with two action potential onsets in several experiments, separated by time delays of up to 2 ms. The first-time derivative of such a signal obtained from the right auricle of a rat heart, for example, is shown in Fig. 5. Single spot measurements, performed earlier, also indicated discontinuities, but could not be interpreted by us



**FIGURE 4** Evidence for discontinuous spread of cardiac excitation. The normalized first-time derivatives of digitally filtered fluorescence signals from photodiodes corresponding to the dotted square in Fig. 2 indicate discontinuous propagation. The fluorescence signal 186 showed two action potential upstrokes, separated by 2.2 ms. Thus, two maxima in the inverted time derivative of signal 186 were found. The neighboring pixels showed their maxima at about the time of either the first or second peak in trace 186. This correspondence in time is pointed out in the overlay plot. A continuous type of propagation transverse to the fiber orientation cannot result in signals like those shown here.

before, due to the lack of information of the excitation in the neighboring areas.

## DISCUSSIONS

Due to propagation velocities of the cardiac impulse in the range of 0.05 to  $>1$  m/s a temporal resolution of  $\sim 100$   $\mu$ s had to be reached for mappings at a microscopic size scale (spatial resolution down to 84  $\mu$ m). The real-time system developed in our laboratory permits recordings of microscopic excitation patterns from beat to beat. Thus, studies of transient changes in the patterns can be performed with this system. This will be of high practical importance

for investigations of irregular dynamics of the heart (e.g., Wenckebach phenomena, flutter, fibrillation). Investigations of the reproducibility, as described in this work, can easily be done in this manner also.

The results shown here represent the summary of cardiac tissue behavior observed in more than 100 experiments. Although such patterns of electrical activity could not be obtained from real-time measurements before, there is increasing evidence that the inhomogeneous and anisotropic distribution of connections between fibers and bundles of fibers, known from light and electron microscopy studies (20), can result in previously unrecognized discontinuous spread of excitation (21). Detailed data of propagation patterns and of the time courses of the action



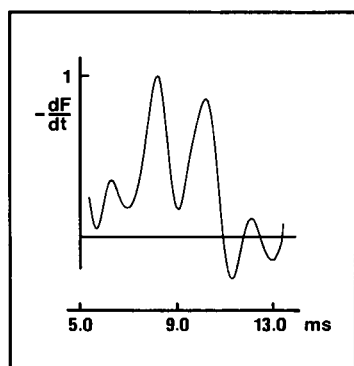


FIGURE 5 Evidence of the discontinuous spread of cardiac excitation within an area of only  $60 \times 60 \mu\text{m}^2$ . The figure shows one of the normalized double-peaked signals measured from the right auricle of a rat. The pattern of excitation across the imaged area ( $1.3 \text{ mm}^2$ ), which is not shown, was very complex, as was the histological structure. Sample time in this experiment was  $64 \mu\text{s}$  for each of the 256 individual signals (4,000,000 samples per second in total).

potential of individual cells of the network, as well as histological studies will be the experimental basis for any progress in this important field of cardiac electrophysiology (22). There is a good chance to reach a spatial resolution of  $\sim 10 \mu\text{m}$ , i.e., the size of single heart muscle cells, by modifying the system introduced here. A commercially available feedback loop with a Pockels cell ("noise eater") can reduce the laser noise by a factor of  $\sim 10$  (11). Objectives with higher magnification will not essentially decrease the signal-to-noise ratio due to the increased numerical aperture associated with higher magnification. Appropriate experiments are currently planned.

Several of the improvements incorporated in our measuring system can be applied profitably to optical measurements of propagation of electrical activity in other tissues. This also holds true for other kinds of fast, simultaneous measurements of multichannel electrical signals.

We thank Dr. L. Loew for the generous gift of the dye and for suggesting its application to cardiac membrane potential measurement.

This investigation was supported by the Austrian Science Research Fund, grant No. P6829-MED.

Received for publication 2 February 1989 and in final form 25 April 1989.

## REFERENCES

1. Cohen, L. B., and B. M. Salzberg. 1978. Optical measurement of membrane potential. *Rev. Physiol. Biochem. Pharmacol.* 83:35–88.
2. Waggoner, A. S. 1979. Dye indicators of membrane potential. *Annu. Rev. Biophys. Bioeng.* 8:47–68.
3. Grinvald, A., R. Hildesheim, J. C. Faber, and L. Anglister. 1982. Improved fluorescent probes for the measurement of rapid changes in membrane potential. *Biophys. J.* 39:301–308.
4. Hassner, A., D. Birnbaum, and L. M. Loew. 1984. Charge-shift probes of membrane potential. *Synthesis. J. Org. Chem.* 49:2546–2551.
5. Windisch, H., W. Müller, and H. A. Tritthart. 1985. Fluorescence monitoring of rapid changes in membrane potential in heart muscle. *Biophys. J.* 48:877–884.
6. Müller, W., H. Windisch, and H. A. Tritthart. 1986. Fluorescent styryl dyes applied as fast optical probes of cardiac action potential. *Eur. Biophys. J.* 14:103–111.
7. Grinvald, A., L. B. Cohen, S. Leshner, and M. Boyle. 1981. Simultaneous optical monitoring of activity of many neurons in invertebrate ganglia using a 124-element photodiode array. *J. Neurophysiol.* 45:829–840.
8. Dillon, S., and M. Morad. 1981. A new laser scanning system for measuring action potential propagation in the heart. *Science (Wash. DC)*. 214:453–456.
9. Ross, W. N., and V. Krauthamer. 1984. Optical measurements of potential changes in axons and processes of neurons of a barnacle ganglion. *J. Neurosci.* 4:659–672.
10. Grinvald, A., E. Lieke, R. D. Frostig, C. D. Gilbert, and T. N. Wiesel. 1986. Functional architecture of cortex revealed by optical imaging of intrinsic signals. *Nature (Lond.)*. 324:361–364.
11. Cohen, L. B., and S. Leshner. 1986. Optical monitoring of membrane potential: methods of multisite optical measurement. In *Optical Methods in Cell Physiology*. P. Weer and B. Salzberg, editors. Wiley-Interscience, New York. 71–99.
12. Grinvald, A. 1986. Real-time optical mapping of a neuronal activity in vertebrate CNS in vitro and in vivo. In *Optical Methods in Cell Physiology*, P. Weer and B. Salzberg, editors. Wiley-Interscience, New York. 165–197.
13. Morad, M., S. Dillon and J. Weiss. 1986. An acousto-optically steered laser scanning system for measurement of action potential spread in intact heart. In *Optical Methods in Cell Physiology*. P. Weer and B. Salzberg, editors. John Wiley & Sons/Interscience, New York. 211–226.
14. Konnerth, A., A. L. Obaid, and B. M. Salzberg. 1987. Optical recording of electrical activity from parallel fibres and other cell types in skate cerebellar slices in vitro. *J. Physiol. (Lond.)* 393:681–702.
15. Shrager, P., S. Y. Chiu, J. M. Ritchie, D. Zecevic, and L. B. Cohen. 1987. Optical recording of action potential propagation in demyelinated frog nerve. *Biophys. J.* 51:351–355.
16. Salama, G., R. Lombardi, and J. Elson. 1987. Maps of optical action potentials and NADH fluorescence in intact working hearts. *Am. J. Physiol.* 252:H384–H394.
17. Kauer, J. S. 1988. Real-time imaging of evoked activity in local circuits of the salamander olfactory bulb. *Nature* 331:166–168.
18. Fluhler, E., V. G. Burnham, and L. M. Loew. 1985. Spectra, membrane binding and potentiometric responses of new charge shift probes. *Biochemistry*. 24:5749–5755.
19. Müller, W., H. Windisch, and H. A. Tritthart. 1987. A refined system to detect cardiac spread of excitation by optical means. In *Proceedings of the 13th Canadian Medical and Biological Engineering Conference*. 233–234.

- 
20. Dolber, P. C. and M. S. Spach. 1987. Thin collagenous septa in cardiac muscle. *Anat. Rec.* 218:45–55.
21. Spach, M. S., W. T. Miller, D. B. Geselowitz, R. C. Barr, J. M. Kootsey, and E. A. Johnson. 1981. The discontinuous nature of propagation in normal canine cardiac muscle. *Circ. Res.* 18:39–54.
22. Spach, M. S., P. C. Dolber, and J. F. Heidlage. 1987. Use of computer simulations for combined experimental-theoretical study of anisotropic discontinuous propagation at a microscopic level in cardiac muscle. *In* *Electro-Mechanical Activation, Metabolism, and Perfusion of the Heart*. S. Sideman, editor. Martinus Nijhoff, Boston. 3–27.